tolerance to the therapy.[8–10] Although patients with HCV-related LC are difficult to treat, patients who achieved SVR showed a lower rate of liver-related adverse outcomes and improved survival.[8–10] Moreover, a randomized controlled trial showed that patients with HCV-related LC who received long-term PEG IFN treatment had a lower risk of HCC than controls.[30] Thus, IFN treatment for HCV-related LC is an effective means of preventing HCC, irrespective of whether SVR is achieved. In this study, the SVR was very low in patients with G1H and the TG or GG allele. Therefore, for these patients, long-term administration of maintenance IFN should be considered to reduce the risk of developing of HCC even if SVR is unlikely to be achieved.

Patients with advanced liver disease have a higher rate of adverse events when taking IFN and ribavirin combination therapy than patients with mild disease. Adverse events, such as neutropenia, thrombocytopenia and anemia, often require dose reduction of IFN or ribavirin. Previous studies have demonstrated that in patients with HCV-related LC, the rate of dose reductions in IFN and ribavirin range 6.9–20.6% and 16.7–27.1%, respectively.[31–33] In our study, IFN and ribavirin dose reductions were needed in 51.3% and 53.6% of patients, respectively. These are higher than those reported in other studies, but the discontinuation rate was slightly lower (12.6%).[33] Many patients required reductions in the doses of IFN and/or ribavirin early in the treatment period because of adverse events, but ultimately were able to tolerate long-term administration. It might be safer to start low-dose antiviral therapy with IFN plus ribavirin in HCV-related LC and titrating the dose upward as tolerated with the aim of long-term treatment, rather than beginning with the full dose and risking adverse events that would curtail antiviral therapy.

In patients infected with HCV genotype 1, previous studies have demonstrated that SVR rates of late virological responders (HCV RNA detectable at 12 weeks and undetectable at 24 weeks after the start of treatment) could be improved when treatment was extended to 72 weeks, compared with the standard treatment duration of 48 weeks, largely as a result of reducing post-treatment relapse rates.[34–37] In this study, the SVR rate in patients who had an LVR was significantly lower than those who achieved RVR or cEVR. However, the duration of treatment in the patients with a LVR was significantly longer than those who achieved cEVR or RVR. Individual physicians determined the duration of treatment based on the time at which serum HCV RNA became undetectable, accounting for the improved SVR rates in those receiving extended courses. Nevertheless, the safety and effectiveness of more than 48 weeks of antiviral therapy in patients with HCV-related LC has not been examined. We found that patients with the IL28B rs8099917 genotype TT, treatment of more than 48 weeks achieved a higher SVR rate than treatment of less than 48 weeks, and in those with the TG or GG alleles SVR rates were greater in those who received more than 72 weeks of treatment. The response to treatment is a very important guide of treatment duration in HCV-related LC. Further prospective studies using larger numbers of patients matched for race, HCV genotype, viral load and treatment durations would be required to explore the relationships between IL28B polymorphism and the treatment response to combination therapy in patients with HCV-related LC.

Recently, new trials of IFN-free combination therapy with direct-acting antivirals (DAA) such as protease-inhibitor, non-structural (NS)5A inhibitor or NS5B polymerase inhibitor nucleotide analog have shown a strong antiviral activity against HCV.[38–40] A previous study reported that the IL28B genotype can affect the response to an IFN-free regimen, but this result has been unclear in other regimens.[38–40] In a study of Japanese patients with HCV genotype 1b infection, dual oral DAA therapy (NS5A inhibitor and NS3 protease inhibitor) without IFN achieved an SVR rate of 90.5% of 21 patients with no response to previous therapy and in 63.6% of 22 patients who had been ineligible for treatment with PEG IFN.[41] However, lack of a virological response to DAA was also seen in patients with no response or partial response to previous therapy. In these patients with viral resistance to DAA, the combination therapy with IFN and DAA may be a means of eliminating HCV, and IL28B genotyping may be a useful tool in determining the best antiviral therapy and duration of treatment.

This study had certain limitations. Selection bias cannot be excluded, considering the retrospective nature of the work. However, all patients had well-established cirrhosis and had received IFN plus ribavirin in hepatitis centers throughout Japan. Our patients received a variety of IFN treatments (IFN-α, IFN-β and PEG IFN), several different doses of IFN and ribavirin, and several treatment durations. In the intention-to-treat analysis, the overall SVR rate was 32.2%; in patients with G1H it was 21.6% but was 60.6% in those with non-G1H. Interestingly, the overall SVR rate in this study was similar to that found in previous studies of patients with advanced fibrosis or cirrhosis treated with IFN or PEG IFN plus ribavirin.[8–10] Thus, although there were some

limitations, our findings contribute to providing valuable information to guide clinical decisions.

In conclusion, the combination therapy with IFN plus ribavirin in Japanese patients with non-G1H HCV-related LC was more effective than those with G1H and not influenced by IL28B polymorphism. However, in patients with G1H, IL28B polymorphism may be a strong predictive factor for SVR. Extending treatment may provide a better outcome in those with the IL28B TT allele treated for more than 48 weeks and in those with the TG/GG alleles treated for more than 72 weeks.

ACKNOWLEDGMENT

THIS STUDY WAS supported by a Grant-in-Aid from the Japanese Ministry of Health, Welfare, and Labor.

REFERENCES

1 Niederau C, Lange S, Heintges T *et al.* Progress of chronic hepatitis C: results of a large, prospective cohort study. *Hepatology* 1998; **28**: 1687–95.
2 Fattovich G, Giustina G, Degos F *et al.* Morbidity and mortality in compensated cirrhosis type C; a retrospective follow up study of 384 paatients. *Gastroenterology* 1997; **112**: 463–72.
3 Hu KQ, Tong MJ. The long-term outcomes of patients with compensated hepatitis C virus-related cirrhosis and history of parenteral exposure in the United States. *Hepatology* 1999; **29**: 1311–16.
4 Sangionvanni A, Prati GM, Fasani P *et al.* The natural history of compensated cirrhosis due to hepatitis C virus: a 17-year cohort study of 214 patients. *Hepatology* 2006; **43**: 1303–10.
5 Nishiguchi S, Kuroki T, Nakatani S *et al.* Randomized trail of effects of interferon-alpha on incidence of hepatocellular carcinoma in chronic active hepatitis C with cirrhosis. *Lancet* 1995; **346**: 1051–5.
6 Shiratori Y, Ito Y, Yokosuka O *et al.* Antiviral therapy for cirrhotic hepatitis C: association with reduced hepatocellular carcinoma development and improved. *Ann Int Med* 2005; **142**: 105–14.
7 Bruno S, Stroffolini T, Colombo M *et al.* Sustained virological response to interferon-alpha is associated with improved outcome in HCV related cirrhosis: a retrospective study. *Hepatology* 2007; **45**: 579–87.
8 Wright TL. Treatment of patients with hepatitis C and cirrhosis. *Hepatology* 2002; **36**: S185–194.
9 Manns MP, McHutchison JG, Gordon SC *et al.* Peginterferon alpha-2b plus ribavirin compared with interferon aalpha-2b plus ribavirin for initial treatment of chronic hepatitis C: a randomized trial. *Lancet* 2001; **358**: 958–65.
10 Bota S, Sporea I, Popescu A *et al.* Response to standard of care antiviral treatment in patients with HCV liver cirrhosis – a systematic review. *J Gastrointestin Liver Dis* 2011; **20**: 293–8.
11 Ge D, Fellay J, Thompson AJ *et al.* Genetic variation in IL28B predicts hepatitis C treatment-induced viral clearance. *Nature* 2009; **461**: 399–401.
12 Tanaka Y, Nishida N, Sugiyama M *et al.* Genome-wide association of IL28B with response to pegylated interferon-alpha and ribavirin therapy for chronic hepatitis C. *Nat Genet* 2009; **41**: 1105–9.
13 Suppiah V, Moldovan M, Ahlenstiel G *et al.* IL28B is associated with response to chronic hepatitis C interferon-alpha and ribavirin therapy. *Nat Genet* 2009; **41**: 1100–4.
14 Ziol M, Handra-Luca A, Kettaneh A *et al.* Noninvasive assessment of liver fibrosis by measurement of stiffness in patients with chronic hepatitis C. *Hepatology* 2005; **41**: 48–54.
15 Castera L, Vergniol J, Foucher J *et al.* Prospective comparison of transient elastography, fibrotest, APRI, and liver biopsy for the assessment of fibrosis in chronic hepatitis C. *Gastroenterology* 2005; **128**: 343–50.
16 Ikeda K, Saitoh S, Kobayashi M *et al.* Distinction between chronic hepatitis and liver cirrhosis in patients with hepatitis C virus infection. Practical discriminant function using common laboratory data. *Hepatol Res* 2000; **18**: 252–66.
17 Ohnishi Y, Tanaka T, Ozaki K, Yamada R, Suzuki H, Nakamura Y. A high-throughput SNP typing system for genome-wide association studies. *J Hum Genet* 2001; **46**: 471–7.
18 Suzuki A, Yamada R, Chang X *et al.* Functional haplotypes of PADI4, encoding citrullinating enzyme peptidylarginie deminase 4, are associated with rheumatoid arthritis. *Nat Genet* 2003; **34**: 395–402.
19 Kawaoka T, Hayes CN, Ohishi W *et al.* Predictive value of the IL28B polymorphism on the effect of interferon therapy in chronic hepatitis C patients with genotype 2a and 2b. *J Hepatol* 2010; **54**: 408–14.
20 Sarrazin C, Susser S, Doehring A *et al.* Importance of IL28B gene polymorphisms in hepatitis C virus genotype 2 and 3 infected patients. *J Hepatol* 2010; **54**: 415–21.
21 Asselah T, De Muynck S, Broët P *et al.* IL28B polymorphism is associated with treatment response in patients with genotype 4 chronic hepatitis C. *J Hepatol* 2012; **56**: 527–32.
22 De Nicola S, Aghemo A, Rumi MG *et al.* Interleukin 28B polymorphism predicts pegylated interferon plus ribavirin treatment outcome in chronic hepatitis C genotype 4. *Hepatology* 2012; **55**: 336–42.
23 Akuta A, Suzuki F, Seko Y *et al.* Association of IL28B genotype and viral response of hepatitis C virus genotype 2 to interferon plus ribavirin combination therapy. *J Med Virol* 2012; **84**: 1593–9.
24 Montes-Cano MA, Garcia-Lozano JR, Abad-Molina C *et al.* Interleukin-28B genetic variants and hepatitis virus

infection by different viral genotypes. *Hepatology* 2010; **52**: 33–7.
25 Yu ML, Huang CF, Huang JF *et al.* Role of interleukin-28B polymorphism in the treatment of hepatitis C virus genotype 2 infection in Asian patients. *Hepatology* 2011; **53**: 7–13.
26 Thomas DL, Thio CL, Martin MP *et al.* Genetic variation in IL28B and spontaneous clearance of hepatitis C virus. *Nature* 2009; **461**: 798–801.
27 Yang M, Rao HY, Feng B, Zhang W, Wei L. The impact of IL28B polymorphisms on spontaneous clearance of hepatitis C virus infection: a meta-analysis. *J Gastroenterol Hepatol* 2013; **28**: 1114–21.
28 Hadziyannis SJ, Sette H Jr, Morgan TR *et al.* Peginterferon-alpha2a and ribavirin combination therapy in chronic hepatitis C: a randomized study of treatment duration and ribavirin dose. *Ann Intern Med* 2004; **140**: 346–55.
29 McHutchison JG, Lawitz EJ, Shiffman ML *et al.* Peginterferon alfa-2b or alfa-2a with ribavirin for treatment of hepatitis C infection. *N Engl J Med* 2009; **361**: 580–93.
30 Lok AS, Everhart JE, Wright EC *et al.* Maintenance peginterferon therapy and other factors associated with hepatocellular carcinoma in patients with advanced hepatitis C. *Gastroenterology* 2011; **140**: 840–9.
31 Fried MW, Shiffman ML, Reddy KR *et al.* Peginterferon alpha-2a plus ribavirin for chronic hepatitis C virus infection. *N Engl J Med* 2002; **347**: 975–82.
32 McHutchison JG, Lawitz EJ, Shiffman , ML *et al.* Peginterferon alfa-2b with ribavirin for treatment of hepatitis C infection. *N Engl J Med* 2009; **361**: 580–93.
33 Bota S, Sporea I, Sirli R *et al.* Severe adverse events during antiviral therapy in hepatitis C virus cirrhotic patients: a systematic review. *World J Hepatol* 2013; **27**: 120–6.
34 Buti M, Valdés A, Sánchez-Avila F, Esteban R, Lurie Y. Extending combination therapy with peginterferon alfa-2b plus ribavirin for genotype 1 chronic hepatitis C late responders: a report of 9 cases. *Hepatology* 2003; **37**: 1226–7.
35 Berg T, von Wagner M, Nasser S *et al.* Extended treatment duration for hepatitis C virus type 1: comparing 48 weeks versus 72 weeks of peginterferon-alfa-2a plus ribavirin. *Gastroenterology* 2006; **130**: 1086–97.
36 Sanchez-Tapias JM, Diago M, Escartin P *et al.* Peginterferon-alfa-2a plus ribavirin for 48 versus 72 weeks in patients with detectable hepatitis C virus RNA at week 4 of treatment. *Gastroenterology* 2006; **131**: 451–60.
37 Akuta N, Suzuki F, Hirakawa M *et al.* A matched case-controlled study of 48 and 72 weeks of peginterferon plus ribavirin combination therapy in patients infected with HCV genotype 1b in Japan: amino acid substitution in HCV core region as predictor of sustained virological response. *J Med Virol* 2009; **81**: 452–8.
38 Poordad F, Lawitz E, Kowdley KV *et al.* Exploratory study of oral combination antiviral therapy for hepatitis C. *N Engl J Med* 2013; **368**: 45–53.
39 Zeuzem S, Soriano V, Asselah T *et al.* Faldaprevir and deleobuvir for HCV genotype 1 infection. *N Engl J Med* 2013; **369**: 630–9.
40 Gane EJ, Stedman CA, Hyland RH *et al.* Nucleotide polymerase inhibitor sofosbuvir plus ribavirin for hepatitis C. *N Engl J Med* 2013; **368**: 34–44.
41 Suzuki Y, Ikeda1 K, Suzuki F *et al.* Dual oral therapy with daclatasvir and asunaprevir for patients with HCV genotype 1b infected and limited treatment options. *J Hepatol* 2013; **58**: 655–62.

Biochimica et Biophysica Acta 1852 (2015) 175–183

Contents lists available at ScienceDirect

Biochimica et Biophysica Acta

journal homepage: www.elsevier.com/locate/bbadis

Hepatic nerve growth factor induced by iron overload triggers defenestration in liver sinusoidal endothelial cells

Lynda Addo [a], Hiroki Tanaka [b,*], Masayo Yamamoto [a], Yasumichi Toki [a], Satoshi Ito [a], Katsuya Ikuta [a], Katsunori Sasaki [b], Takaaki Ohtake [a], Yoshihiro Torimoto [c], Mikihiro Fujiya [b], Yutaka Kohgo [a]

[a] Division of Gastroenterology and Hematology/Oncology, Asahikawa Medical University, Asahikawa, Hokkaido, Japan
[b] Department of Gastrointestinal Immunology and Regenerative Medicine, Asahikawa Medical University, Asahikawa, Hokkaido, Japan
[c] Oncology Center, Asahikawa Medical University Hospital, Asahikawa, Hokkaido, Japan

ARTICLE INFO

Article history:
Received 3 July 2014
Received in revised form 13 November 2014
Accepted 17 November 2014
Available online 21 November 2014

Keywords:
NGF
Iron
Liver sinusoidal endothelial cells
Defenestration

ABSTRACT

The fenestrations of liver sinusoidal endothelial cells (LSECs) play important roles in the exchange of macromolecules, solutes, and fluid between blood and surrounding liver tissues in response to hepatotoxic drugs, toxins, and oxidative stress. As excess iron is a hepatotoxin, LSECs may be affected by excess iron. In this study, we found a novel link between LSEC defenestration and hepatic nerve growth factor (NGF) in iron-overloaded mice. By Western blotting, NGF was highly expressed, whereas VEGF and HGF were not, and hepatic NGF mRNA levels were increased according to digital PCR. Immunohistochemically, NGF staining was localized in hepatocytes, while TrkA, an NGF receptor, was localized in LSECs. Scanning electron microscopy revealed LSEC defenestration in mice overloaded with iron as well as mice treated with recombinant NGF. Treatment with conditioned medium from iron-overloaded primary hepatocytes reduced primary LSEC fenestrations, while treatment with an anti-NGF neutralizing antibody or TrkA inhibitor, K252a, reversed this effect. However, iron-loaded medium itself did not reduce fenestration. In conclusion, iron accumulation induces NGF expression in hepatocytes, which in turn leads to LSEC defenestration via TrkA. This novel link between iron and NGF may aid our understanding of the development of chronic liver disease.

1. Introduction

Liver sinusoidal endothelial cells (LSECs) are unique endothelial cells both morphologically and functionally. These cells line hepatic sinusoids and thus play important roles in regulating hepatic microcirculation. They also lack a basement membrane and are characterized by fenestrae, which occupy 6-8% of the endothelial surface [1–4] and act as dynamic filters that play an active role in regulating the exchange of macromolecules, solutes, and fluid between the blood and the surrounding tissues [5–7]. However, in disease states, the diameter and number of LSEC fenestrae undergo changes, such as loss of fenestrae (defenestration), in both animals and humans [8–17]. These changes can be induced by several factors, including drugs and toxins [18–22], and are believed to have adverse effects on liver function in general [4]. However, the precise mechanism by which these hepatotoxins induce defenestration remains to be elucidated. Iron, a vital requirement for normal cellular function, is also an important hepatotoxin when present in excess, which may affect endothelial cell function and induce defenestration.

It is well known that growth factors, such as hepatocyte growth factor (HGF), tumor necrosis factor (TNF), and interleukin-6 (IL-6), are involved in hepatic regeneration [24]. Furthermore, neurotrophins (NTs) may play a role in hepatic regeneration [25–27]. Nerve growth factor (NGF), a member of the NT family, is the most expressed NT in the adult mouse liver [28]. NGF is also proapoptotic in the liver [27] and is thought to protect the liver against oxidative stress and xenobiotic injury [29]. NGF was also shown to be highly expressed in hepatocytes and hepatoma cells in liver cirrhosis and hepatocellular carcinoma in both clinical [30, 31] and animal models [26,27], which suggests that NGF may contribute to the pathophysiology of liver disease. Thus, in the present study, we focused on the link between hepatic iron overload and NGF expression using mouse models of iron overload.

2. Materials and methods

2.1. Animals

Male C57Bl/6 mice (Clea Japan, Tokyo, Japan) were randomly assigned to three treatment groups: control, dietary iron (slight

* Corresponding author at: Department of Gastrointestinal Immunology and Regenerative Medicine, Asahikawa Medical University, 2-1-1-1 Midorigaoka-Higashi, Asahikawa, Hokkaido 078–8510, Japan.
E-mail address: hiroki-t@asahikawa-med.ac.jp (H. Tanaka).

http://dx.doi.org/10.1016/j.bbadis.2014.11.014
0925-4439/

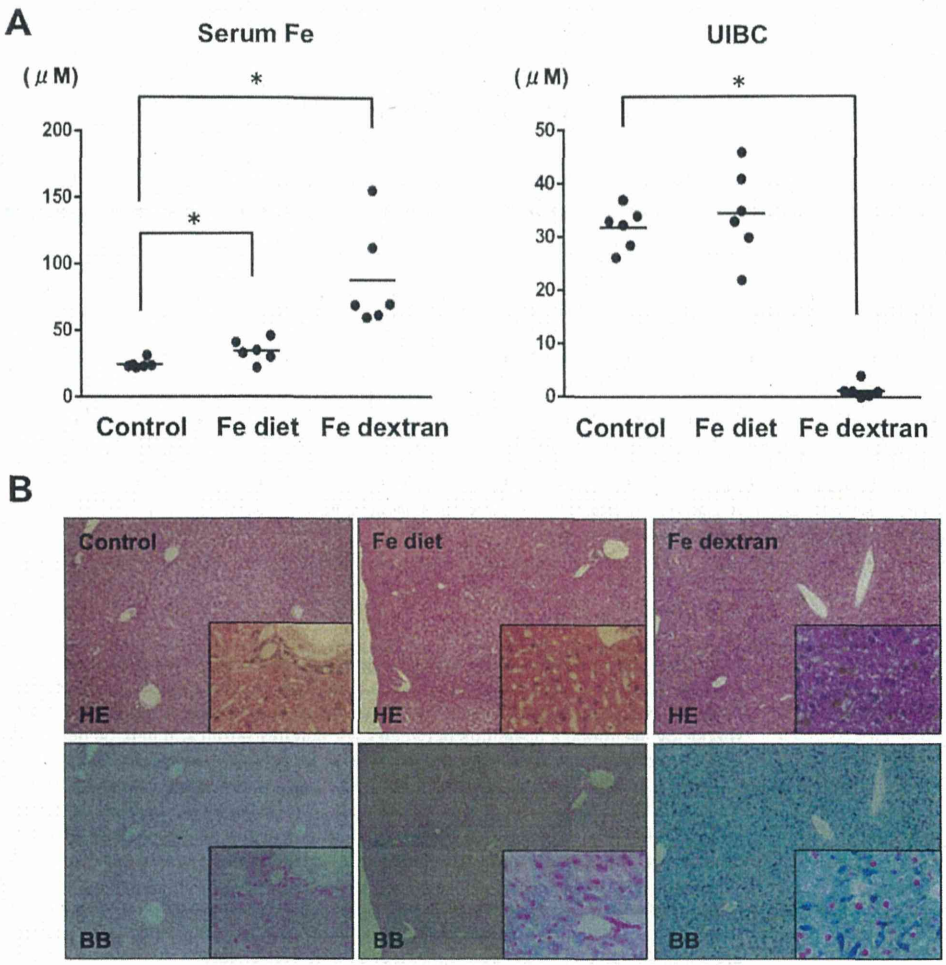

Fig. 1. Serum and histologic evidence of iron overload. (A) Serum iron was slightly increased in the iron diet group but significantly increased in the iron dextran group. However, UIBC was significantly reduced. (B) Slight iron accumulation was observed in the portal area of iron diet mice, with severe iron accumulation observed throughout the liver tissues of iron dextran mice (*$P < 0.05$). H&E staining shown in the upper row, Berlin Blue staining shown in the lower row.

iron overload), and iron dextran (severe iron overload). Each group comprised five mice. The control group was fed a regular mouse chow diet for 8 weeks, while the dietary iron overload group was fed a 2.5% (w/w) carbonyl iron diet for 8 weeks. The iron dextran group received intraperitoneal injections of iron dextran solution (10 mg iron/head/day) (Sigma-Aldrich, St. Louis, MO, USA) for 5 days. Another group of five mice received intraperitoneal injections of mouse recombinant NGF (1 μg/head/day) (Promega, Madison, WI, USA) for 3 days. The mice were sacrificed at the end of each treatment period, and serum and liver tissues were collected. The liver tissues were processed for formalin-fixed paraffin-embedded tissue blocks and then subjected to H&E and Berlin Blue staining. All animal experiments were approved by the animal experiments committee of the Asahikawa Medical University (Hokkaido, Japan) based on guidelines for the protection of animals.

2.2. Serum analysis

Serum iron and unsaturated iron binding capacity (UIBC) were measured with the automatic serum analyzer LABOSPECT 008 (Hitachi, Tokyo, Japan). Assay reagents were obtained from Shino-Test (Tokyo, Japan).

2.3. Western blotting

Liver tissues were lysed in RIPA buffer, separated in polyacrylamide gels and electro-transferred to nitrocellulose membranes. After blocking with 5% nonfat dry milk in PBST buffer (PBS containing 0.05% Tween-20), the membranes were probed with rabbit anti-NGF (Abcam, Cambridge, UK), rabbit anti-HGF (Abcam), mouse anti-VEGF (Santa Cruz Biotechnology, Santa Cruz, CA, USA), rabbit anti-TrkA (Novus Biologicals, Littleton, CO, USA), or mouse anti-Actin antibody (BD Bioscience, Franklin Lakes, NJ, USA). The membranes were then incubated with the respective HRP-conjugated anti-mouse or anti-rabbit IgG secondary antibodies (R&D Systems, Minneapolis, MN, USA). Antibody binding was visualized using the SuperSignal West Pico Chemiluminescent Substrate (Thermo Scientific, Waltham, MA, USA).

2.4. Digital PCR analysis

Absolute copy numbers of mouse Ngf mRNA were analyzed using the digital PCR system with the TaqMan probe for mouse *Ngf* (Life Technologies, Carlsbad, CA, USA). RNA was extracted from the livers using the Purelink RNA mini kit (Life Technologies), and the RNA concentrations were measured by fluorometric quantification using

the Qubit 2.0 (Life Technologies). Reverse transcription using a high-capacity complementary DNA reverse transcription kit (Life Technologies) was then performed. PCR results were analyzed using the QuantStudio 3D Digital PCR system (Life Technologies).

2.5. Cell isolation and culture

Primary hepatocytes and LSECs were isolated from healthy, untreated C57Bl/6 mice using the *in situ* collagenase perfusion method [32]. Primary hepatocytes were cultured in William's E medium (supplemented with 10% FBS, 0.1 μmol/L EGF and 0.1 μmol/L insulin) (Sigma-Aldrich), while primary LSECs were cultured in DMEM (supplemented with 10% FBS and penicillin streptomycin) (Wako, Tokyo, Japan) overnight. The primary hepatocytes were then treated with holo-transferrin (3 mg/mL and 6 mg/mL) conjugated with Alexa Fluor 594 (Invitrogen, Carlsbad, CA, USA) and ferric ammonium citrate (FAC) (1 μM and 5 μM) (Sigma-Aldrich) for 24 h. For electron microscopy, LSECs were treated with mouse recombinant NGF (5 ng/mL) (Promega), mouse anti-NGF neutralizing antibody (1 μg/mL) (Millipore, Temecula, CA, USA), and K252a, the TrkA inhibitor (5 ng/mL) (LC Laboratories, Woburn, MA, USA). For the MTT assay (Promega), primary LSECs were cultured with 0, 1, 5, and 10 ng/mL mouse recombinant NGF (Promega) for 24 and 48 h, and the cell growth activity was measured according to the manufacturer's protocol.

2.6. Immunohistochemistry and Immunofluorescence

After deparaffinization, rehydration, and antigen retrieval, the tissue sections were first incubated with anti-NGF rabbit polyclonal antibody (Abcam, Cambridge, UK) and anti-TrkA rabbit polyclonal antibody

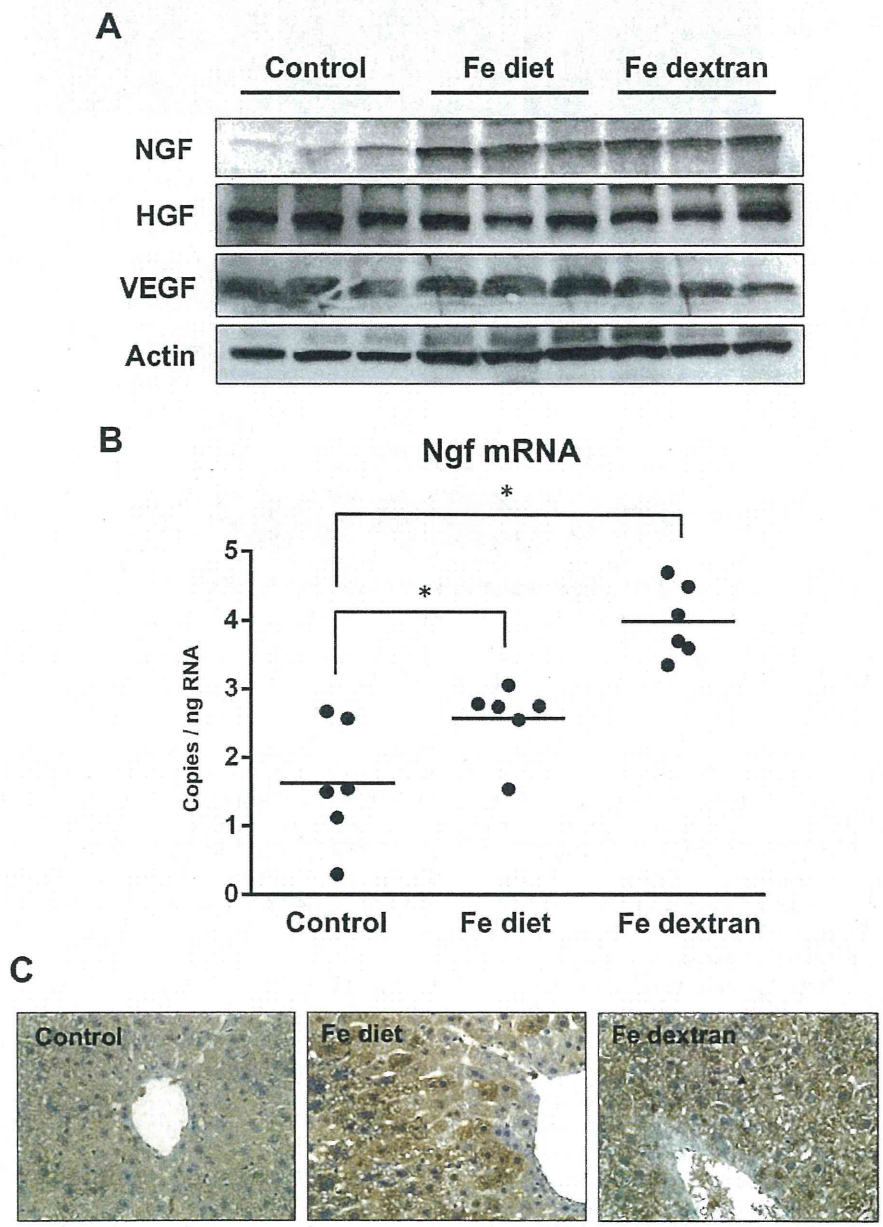

Fig. 2. NGF is highly expressed in the liver following iron overload. (A) Western blot analysis for NGF, HGF, and VEGF. (B) Ngf mRNA analysis (*$P < 0.05$). (C) Immunohistochemistry for NGF in mouse liver tissues.

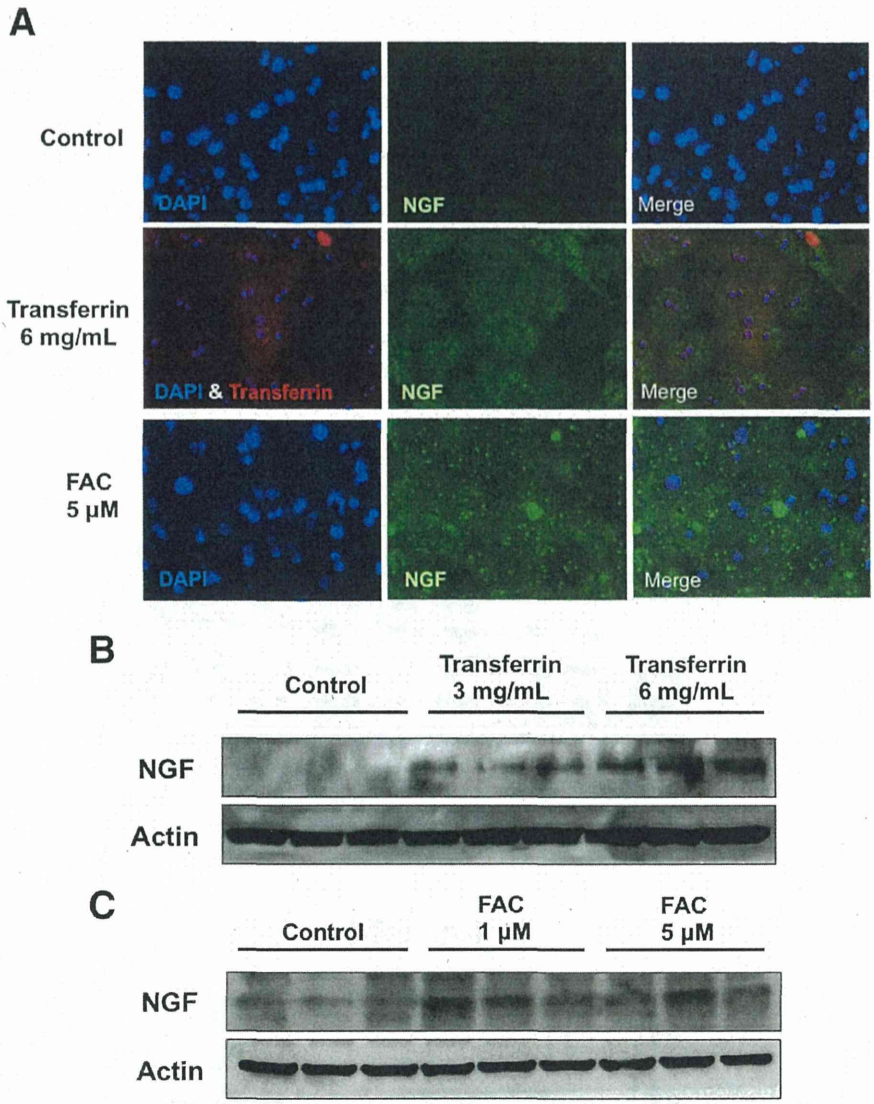

Fig. 3. Primary hepatocytes express NGF following iron overload. (A) NGF expression in primary hepatocytes cultured in pre-conditioned iron overload medium (Alexa Fluor 594-conjugated holo-transferrin and FAC) (×400 original magnification) for 24 h. Western blotting in (B) holo-transferrin (3 mg/mL and 6 mg/mL)- and (C) FAC (1 μM and 5 μM)-treated samples.

(Novus Biological, Littleton, CO, USA). Antibody binding was visualized with the HRP-conjugated secondary antibody system ImmPRESS reagent (Vector Labs, Burlingame, CA, USA). Primary hepatocytes and LSECs were fixed in 4% paraformaldehyde and then incubated with anti-NGF (Abcam) and anti-VE-cadherin (Abcam) antibodies, respectively. The samples were then incubated with Alexa Fluor 488-conjugated anti-rabbit IgG antibody (Invitrogen), followed by nuclear staining with 4′,6-diamidino-2-phenylindole (DAPI). Fluorescent microscopy was performed with a BZ-9000 microscope (Keyence, Osaka, Japan).

2.7. Scanning electron microscopy

After the mice were sacrificed, the livers were cannulated via the portal vein and fixed in 2.5% glutaraldehyde. The livers were then collected and cut into small blocks, which were then fixed in 4% osmium for 1 h. The livers were then processed for sequential alcohol dehydration and infiltrated with t-butyl alcohol. After freezing, the tissues were vacuum-dried and then coated with ion sputter Hitachi E-1030 (Hitachi, Tokyo, Japan) for analysis with the scanning electron microscope SEM S-4100 (Hitachi). For isolated primary LSECs, the cells were plated on collagen-coated cell culture inserts (BD Biosciences, Bedford, MA), cultured overnight, and treated for 24 h as described in the Cell Isolation and Culture section. Membranes of the cell culture inserts containing cells were then processed using the same procedures described above. For quantification of fenestrae in liver sinusoids or primary LSECs, the number of fenestrae (per μm^2) was analyzed with Image J (NIH, Bethesda, Maryland, USA).

2.8. Statistics

The Student's paired *t*-test was used. $P < 0.05$ was considered statistically significant.

3. Results

3.1. Serum and histologic evidence of slight and severe iron overload in experimental animals

The serum iron concentration in the iron diet group (slight iron overload) was slight but statistically significant. However, in the iron

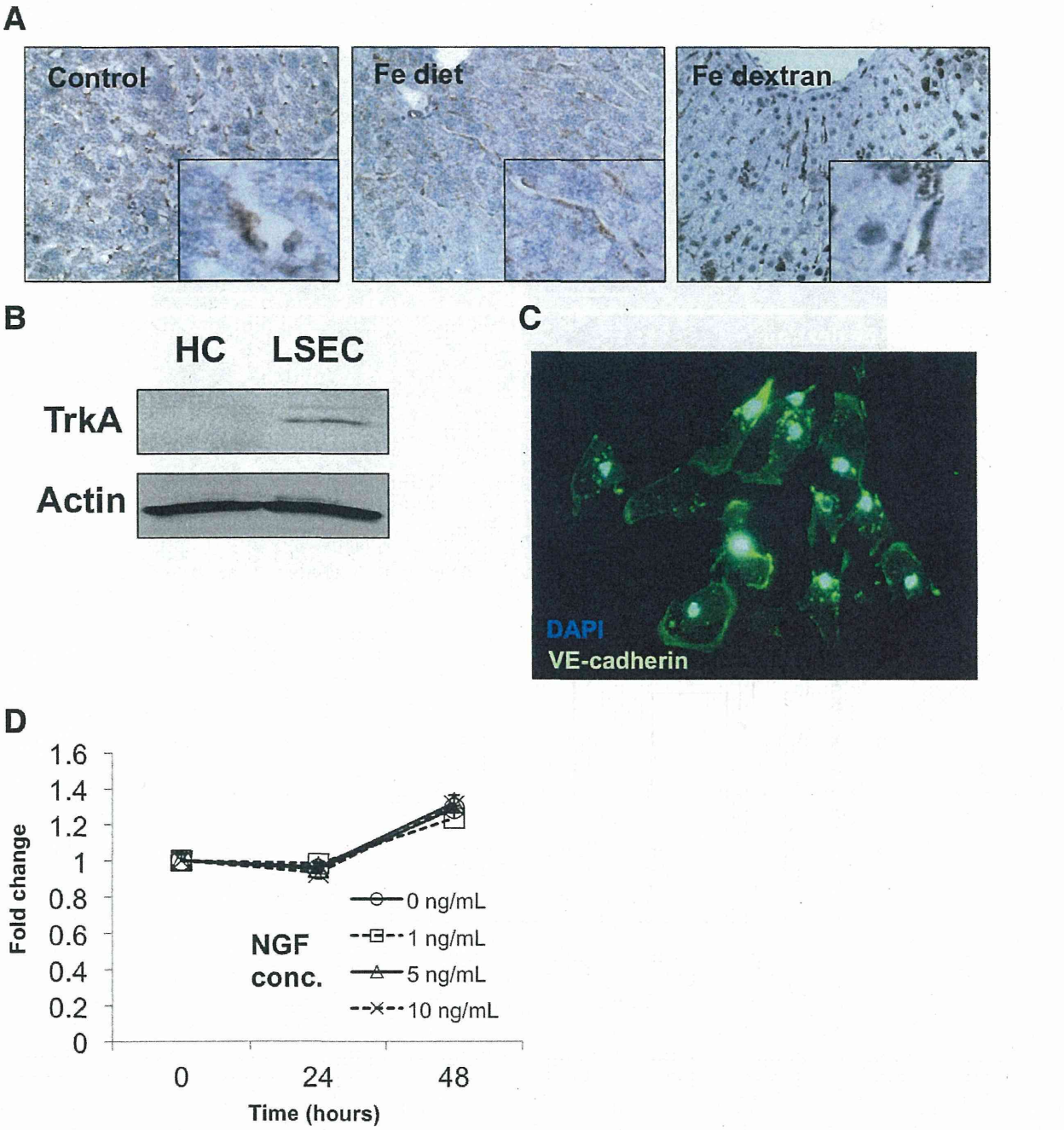

Fig. 4. LSECs express TrkA. (A) TrkA (brown staining) expression in LSECs. (B) Western blotting for TrkA expression in hepatocytes (HC) and LSECs. (C) Positive staining for VE-cadherin (green) in isolated LSECs. (D) Growth assay in primary isolated LSECs cultured with mouse recombinant NGF.

dextran group (severe iron overload), the serum iron level was significantly increased, while UIBC was significantly decreased (Fig. 1A). Histologic evidence of hepatocellular iron in the iron diet group was mild and subtle with only slight iron accumulation in hepatocytes in the portal area, while hepatocellular iron in the iron dextran group was severe, with clear evidence of iron accumulation in the entire liver tissue (Fig. 1B).

3.2. Hepatocytes express NGF during iron overload

By Western blotting, mouse NGF expression was up-regulated in the livers of both iron overload models, while the expression of HGF and VEGF, two important hepatic growth factors, did not show any significant change (Fig. 2A). Digital PCR analysis of absolute mRNA copy numbers showed that *Ngf* mRNA expression was significantly up-regulated in both iron overload models (Fig. 2B). Of note, *Ngf* expression was significantly up-regulated even in the slight iron overload liver, which showed no histological evidence of inflammation or cellular damage. This observation indicates that *Ngf* expression may serve as an early event during iron accumulation. Immunohistochemistry further showed that NGF protein was localized in hepatocytes (Fig. 2C).

3.3. Primary hepatocytes express NGF in iron overload conditioned medium

To confirm the cellular source of NGF expression in the liver, immunofluorescence staining of primary hepatocytes cultured in pre-conditioned

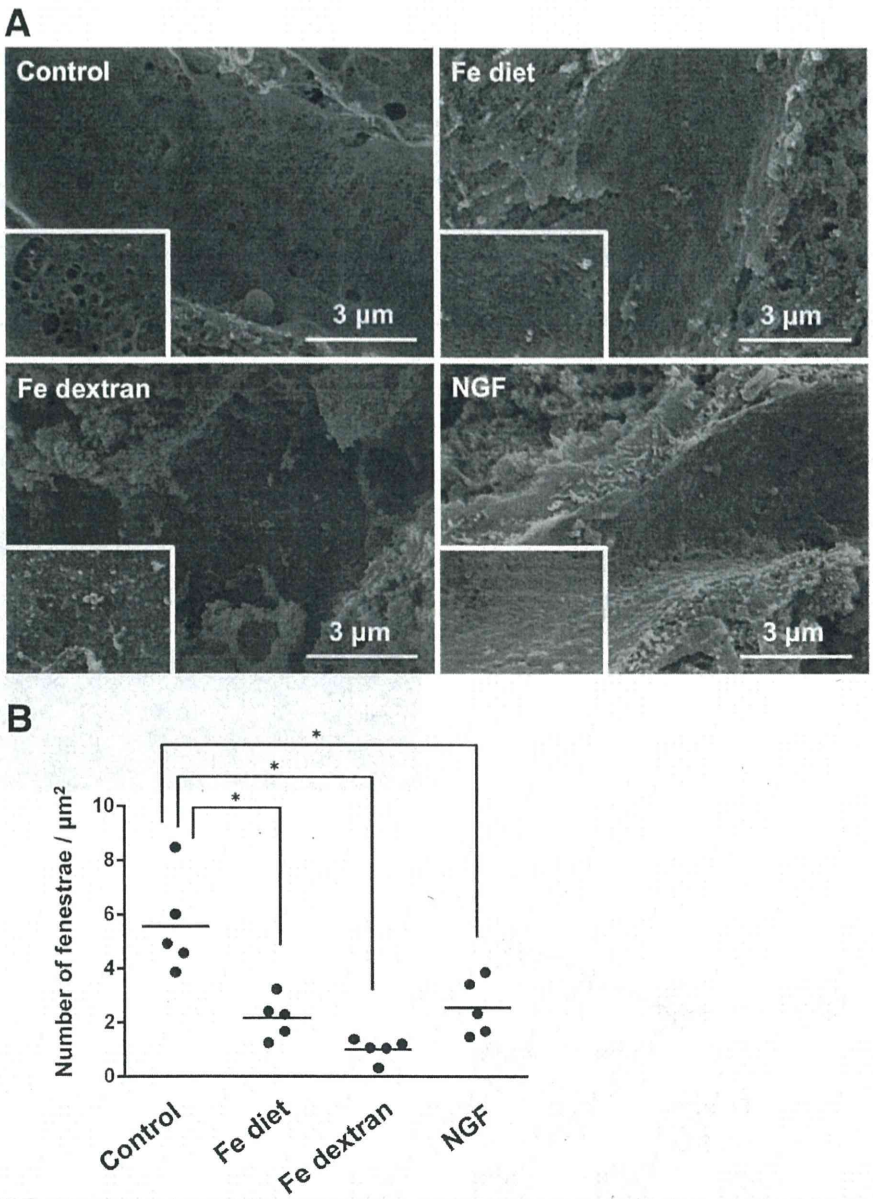

Fig. 5. SEM in mouse liver tissue. (A) LSEC fenestrae (insert) were clearly visible in control tissues (SEM ×10,000 magnification). LSEC fenestration was absent in iron diet and iron dextran livers. Defenestration was also observed in LSECs after NGF treatment. The pictures shown for each treatment group represent one picture selected from a total of five representative images. (B) Graph showing the number of fenestrae per μm^2.

iron overload medium, as described in the Materials and Methods section, was performed. NGF expression was up-regulated in primary hepatocytes in both the holo-transferrin (6 mg/mL) and FAC-treated samples (5 μM) (Fig. 3A), and this finding was further confirmed with Western blotting (Fig. 3B and C).

3.4. LSECs express TrkA

As NGF mainly signals through the high-affinity tyrosine kinase-coupled receptor TrkA, we characterized the expression of this receptor. By immunohistochemical staining, TrkA was positively expressed in LSECs following iron overload (Fig. 4A). Western blotting for the mouse TrkA antibody in primary isolated LSECs, and hepatocytes confirmed the expression of TrkA in LSECs but not in hepatocytes (Fig. 4B). Immunofluorescence staining showed intense staining for VE-cadherin, an endothelial cell marker, in isolated LSEC membranes (Fig. 4C). Because isolated primary LSEC growth is reported to be stimulated by growth-promoting substances secreted from cultured hepatocytes [33], we also investigated whether recombinant NGF had any growth effect on LSECs. However, we found that mouse recombinant NGF did not affect the growth of LSECs *in vitro* (Fig. 4D).

3.5. LSEC fenestration is lost during iron overload

Using high-performance scanning electron microscopy (SEM), we investigated whether iron overload induced any morphological changes in the liver. While sieve plate structures (fenestrae) were present in the liver sinusoids of control mice, fenestration was not present in both iron overload models (Fig. 5A, B). Interestingly, this same phenomenon

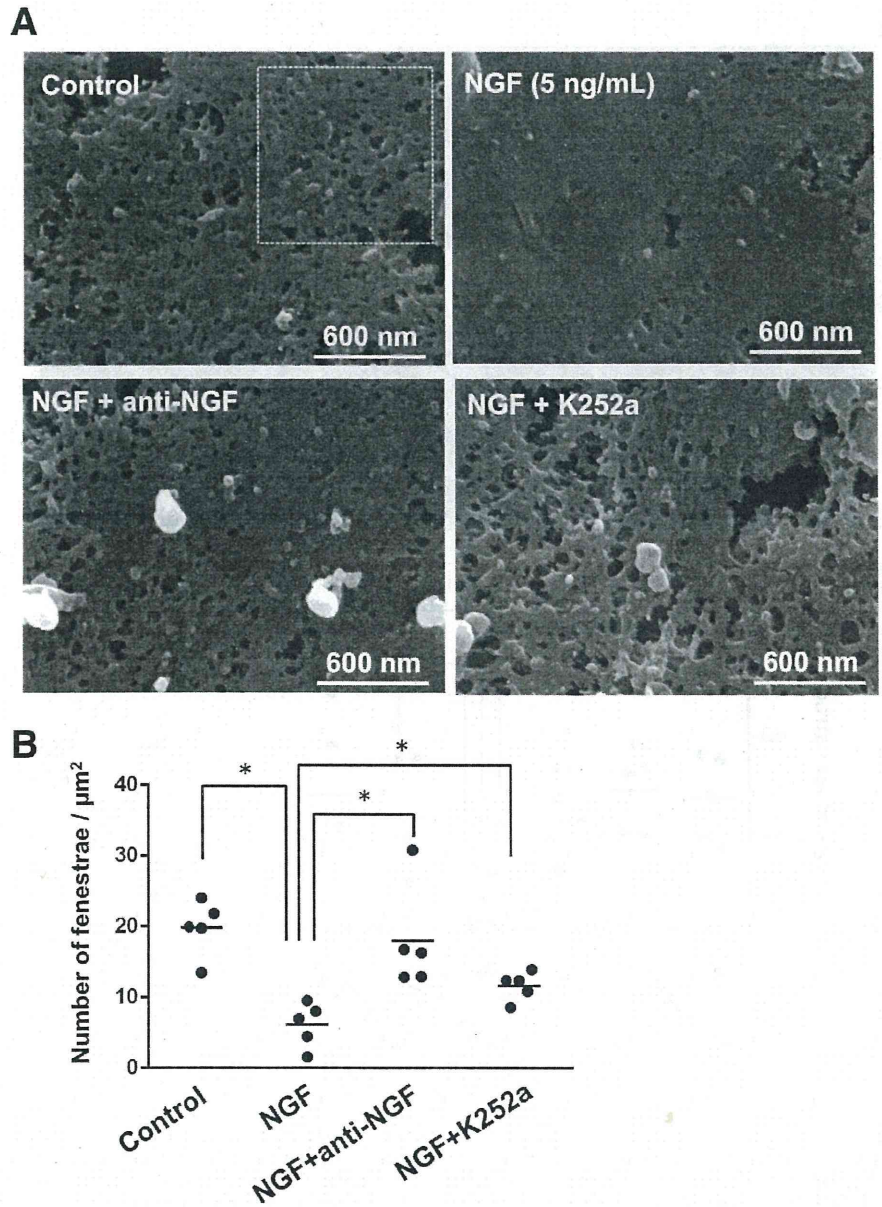

Fig. 6. SEM in isolated LSECs. (A) Mouse recombinant NGF (5 ng/mL) reduced LSEC fenestration, whereas treatment with an anti-NGF neutralizing antibody or the TrkA inhibitor, K252a, reversed this effect (SEM ×50,000 magnification). The white dotted line in the control image represents a 1 μm^2 area. (B) Graph showing the number of fenestrae per μm^2. The pictures shown for each treatment group represent one picture selected from a total of five representative images. Anti-NGF: NGF neutralizing antibody. K252a: TrkA inhibitor.

(defenestration) was observed when mice were intraperitoneally injected with mouse recombinant NGF (Fig. 5A, B).

3.6. NGF reduces fenestration in LSECs

To investigate the hypothesis that NGF may be responsible for the defenestration observed, mouse primary LSECs were isolated and cultured with mouse recombinant NGF, after which SEM was performed. The results showed evidence of defenestration (Fig. 6A, B), although subsequent incubation with an anti-NGF neutralizing antibody or TrkA inhibitor (K252a) reversed this defenestration effect (Fig. 6A, B).

3.7. Iron does not directly influence LSEC fenestration

To assess whether or not iron was responsible for the defenestration observed, primary LSECs were cultured in fresh iron overload medium (6 mg/mL holo-transferrin and 5 μM FAC) for 24 h. Defenestration was not observed in this experiment (Fig. 7A, C). Mouse hepatocytes were then cultured in iron overload medium (6 mg/mL holo-transferrin) for 24 h, and the supernatant was collected. When this pre-conditioned supernatant medium was cultured with mouse primary LSECs, LSEC fenestration was reduced, and treatment with an anti-NGF neutralizing antibody or TrkA inhibitor (K252a) reversed this effect (Fig. 7B, C). These observations clearly indicate that iron stimulated NGF secretion from hepatocytes, which then induced LSEC defenestration.

4. Discussion

Our study demonstrates that NGF is highly expressed under conditions of both severe and slight iron overload in mice, suggesting a possible role for NGF in hepatic iron loading. We also observed intense staining for NGF in hepatocytes, which indicates that hepatocytes are